

STRAW TUBE SUBSYSTEM OF THE CBM MUON DETECTOR

*V. Peshekhonov, A. Baskakov, N. Grigalashvili, G. Kekelidze,
V. Lysan, V. Myalkovskiy, D. Peshekhonov, S. Rabtsun, A. Zinchenko*

Joint Institute for Nuclear Research, Dubna

A straw tube subsystem design of the muon detector of the Compressed Baryonic Matter (CBM) experiment is described. Main parameters of the subsystem are shown. The muon detector performance evaluation results obtained using the Monte Carlo simulation are presented.

Представлено описание подсистемы мюонного детектора эксперимента CBM, основанной на строу-трубках. Приведены основные параметры подсистемы. Проведена оценка характеристик мюонного детектора с использованием моделирования Монте-Карло, и представлены основные результаты.

PACS: 29.40.Gx

INTRODUCTION

CBM Muon Detector (MUCH) should provide an identification of muons in heavy-ion collisions at FAIR energies [1]. The detector consists of several hadron absorber layers with intermediate gas tracking detectors. The coordinate detectors will be used for tracking of charged particles produced at scattering angles from 5.7 to 26.6°. The general view of the proposed muon system is presented in Fig. 1. Tracking detectors based on drift tubes will be used for the two last gaps of the absorber layers (stations 4 and 5). To ensure the low occupancy and high uniformity of the detector, it is planned to make use of thin-walled 6 mm straws for these tracking stations as described in the next Section.

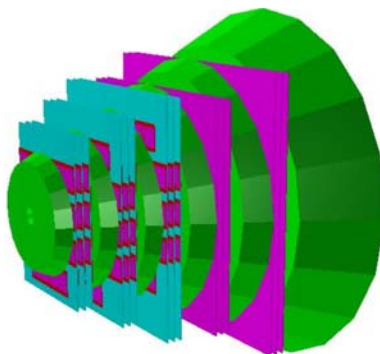


Fig. 1. CBM muon system configuration with thin-walled drift tubes (straws): straw detector stations are placed behind absorbers 4 and 5

1. STRAW TUBE SYSTEM DESIGN AND MECHANICAL STRUCTURE

1.1. Design of the Straw Detector Station. Each straw station contains three identical octagonal chambers measuring X and two rotated $(+10, -10)$ coordinates of a passing charged particle. Each chamber consists of two identical modules with some overlap between them to avoid dead regions. The chambers have an inner hole for the beam pipe with a diameter of 43 cm. Figures 2 and 3 show the schematic layout of the straw module and the straw chamber, respectively.

Each module contains two layers of straws of a length from 84 to 190 cm (for station 5) which are inserted into a carbon frame. The straws of one layer are glued together to form a plane. Every plane is divided into three sections. The central part, being closer to the beam

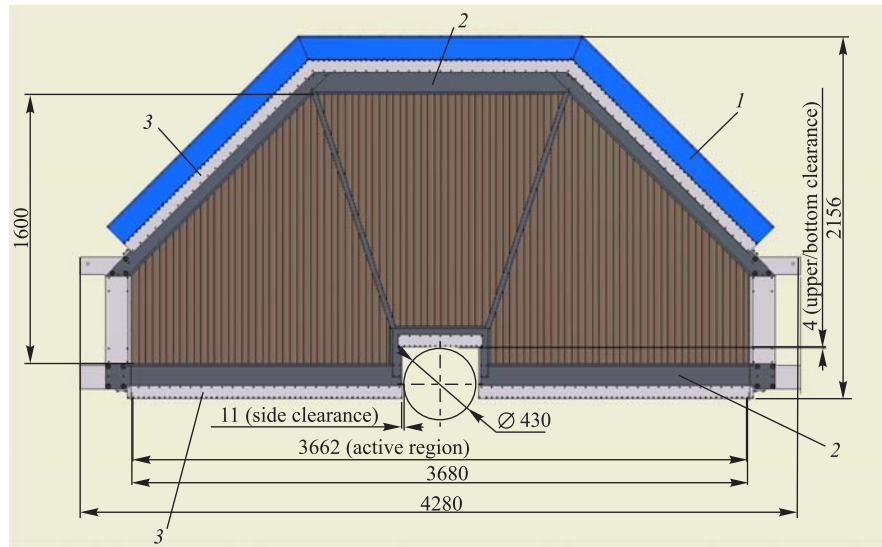


Fig. 2. Schematic view of the MUCH straw module. 1 — mother boards for the readout and high voltage supply of the straw anodes; 2 — carbon plastic elements, and 3 — Al elements

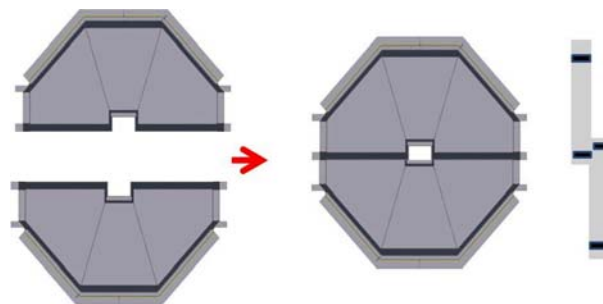


Fig. 3. Schematic view of the MUCH straw chamber

axis, is exposed to higher rates. This part has a central half-hole for the beam pipe. Each layer has 592 straws with 6.0 mm inner diameter. The chosen diameter is a compromise between minimizing the number of channels and value of the occupancy. A plane of this kind has a much higher mechanical stability compared to individual straws. This improves the ruggedness and reduces the load onto the frame, which would be needed to keep individual straws straight enough by tension. The production technology was developed for the straw subsystem of the COMPASS spectrometer [2–4] and used for the different size chambers of the setup SVD-2 and OKA of the U-70 accelerator at IHEP (Protvino).

Two straw planes are combined into one double layer and mounted on two transverse to the straw direction carbon bars of the frame as shown in Fig. 2. Utilization of the carbon plastic for these bars is preferable because of relatively large temperature expansion coefficient for Al. Aluminium bars were used for the other direction and as a support of the mother boards, etc.

One layer of the straws is shifted by half a diameter with respect to the other in order to resolve left-right ambiguities. The anode wires of the drift tubes are centered in the straws by two end-plugs and one or two small plastic spacers. The diameter of these gold-plated tungsten wires is 30 μm . The ends of the straws of a double layer are glued gas tight on each side of the frame, which serves at the same time as a part of the gas manifolds. The straws are supplied with the counting gas through the end-plugs and the gas manifolds.

The length of the straw tubes is affected by humidity. In order to keep the straw tubes straight and exclude any possibility of the straw bending, they can be reinforced by carbon

Table 1. Some parameters of the straw stations 4 and 5

Station No.	R_{out} of station, cm	Station thickness, cm	Straw diameter, mm	Max. drift time, ns	Intrinsic spatial resolution, μm	Max. occupancy, %	N_{straw} /module
4	159	30	6.0	60	170	< 7	1024
5	185	30	6.0	60	170	< 2	1184

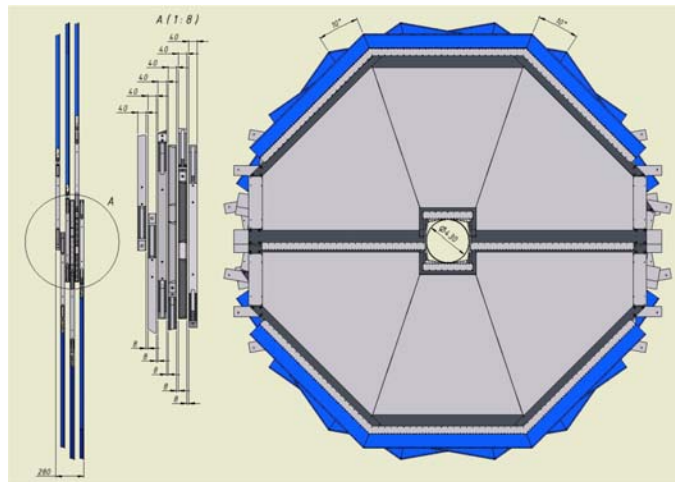


Fig. 4. Schematic view of the MUCH station with three chambers

wires like it was done for the ATLAS TRT. But the long straws should be installed into the frame under a small pre-tension and kept under low humidity. In order to minimize the effects of humidity, the straw planes will be closed by thin Al planes from both module sides to provide the possibility to surround the straws by a dry gas. The additional construction elements will include mother and termination boards, which will be located near outer and inner straw ends, respectively.

Some parameters of the stations are presented in Table 1, and schematic view of the MUCH station is shown in Fig. 4. The gas mixture will be Ar/CO₂ (70/30), and the gas gain will be $\sim 5 \cdot 10^4$. The average intrinsic spatial resolution of the straw is about 170 μm .

1.2. Straws. The structure of a straw tube is shown in Fig. 5. The straws for the prototype are wound from two Kapton film strips. Carbon-loaded Kapton film of the 160 XC 370 type from DUPONT and aluminized (500 Å) Kapton film of the NH type will be used as inner and outer strips, respectively. Both films will be covered by a glue layer with a thickness



Fig. 5. Straw tube consisting of a carbon-loaded inner layer 40 μm thick and an aluminized Kapton outer layer $\sim 25 \mu\text{m}$ thick

of 7 μm on one their side. The inner diameter of the straws will be 6 mm and the tolerance of the diameter was specified to $0 + 30 \mu\text{m}$.

Radiation hardness properties of the Kapton XC had been tested before for the COMPASS straw tracker. The aging properties of straws were studied with 26-MeV proton beams from the Munich Tandem accelerator. In addition, the experience of the COMPASS experiment shows good aging properties of similar straws [5].

During the module assembly some other internal straw components will be required. The gold-plated tungsten–rhenium wire with a 30 μm diameter (type 861, Luma) will be used as an anode. The wire under 70 grams tension is fixed by the crimp pins inserted in the polycarbonate end-plugs. The diameter of the end-plugs is 6.0–0.018 mm. In order to decrease the wire displacement due to electrostatic and gravitational forces, spacers will be placed with the distance between them no more than 700 mm. The spacers are produced of polycarbonate by pressure molding. Their design is optimized in order to reduce the insensitive zone. The spacer diameter is 5.97–0.018 mm, the length along the anode wire is ~ 1 mm and mass is 15 mg.

1.3. Electrical Periphery. A simplified schematic circuit of one detector channel is shown in Fig. 6. The signal readout will be organized from one (outer) end of the tube. In order to avoid pulse reflections, a proper termination of both ends of anode wires is foreseen. A serial resistor at the amplifier input together with the input resistance of the amplifier should provide the right impedance for the termination on the readout side of a straw. The inner ends will be connected to the termination boards (TB), where 100 pF capacitors will be used between anodes and termination resistors of 330 Ω . The TB contains a test pulse line for testing of the full readout chain. The general view of the prototype TB is shown in Fig. 7.

The motherboards (MB) will feed the anode voltage to and read the information from the straws on both module planes, and will be mounted on Al elements of the frame on the outer side of the chamber, while TBs for the straw anode termination will be mounted on the opposite side. The octagonal shape of the chamber requires several different types of MBs as

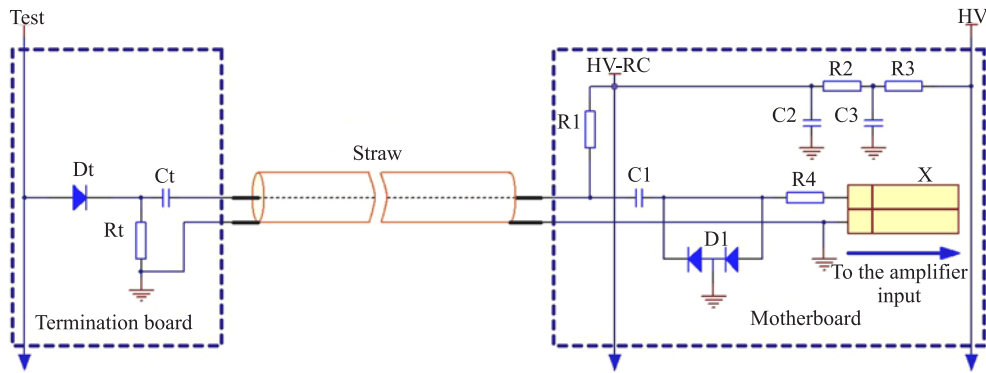


Fig. 6. A simplified TB and MB circuit diagram for one channel

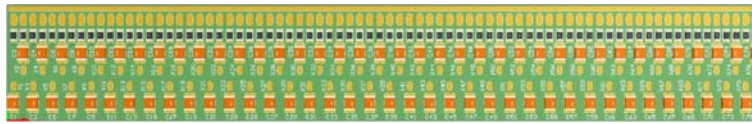


Fig. 7. General view of one TB

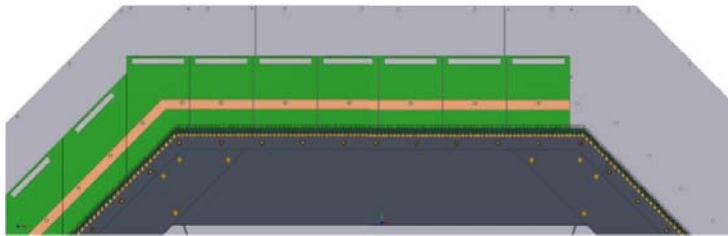


Fig. 8. Two fragments with the mounted MB on left and center parts of the module prototype

can be seen in Fig. 8. The MB contains also a coupling between straw tubes and amplifiers and HV protection diodes for the amplifier inputs. The MB buses also provide a conductive coupling of the straw cathodes to the appropriate ground buses of FEE. Both printed circuit boards (MBs and TBs) are produced in a multilayer technology. Some details of different types of MBs are shown in Figs. 9 and 10.

To achieve the tracking performance desired, the readout electronics has to amplify the incoming straw signals and to perform the following functions:

- shape the amplified signal and remove the ion tail;
- apply a threshold to detect MIP with proper spatial resolution and store in a pipeline the timing information for the accepted signal;
- gather and compress in a readout driver (ROD) the data from many channels, format and send them to the readout buffer.

The analogue bipolar ASIC should provide eight channels of amplifier, shaper, discriminator and baseline restorer, similar to the one used in ATLAS TRT [6]. The dynamic range for the threshold should be from 2 to 15 fC with an operation threshold of ~ 3 fC (300 eV) with uniformity $\pm 15\%$. The signal peaking time should be 5–8 ns, and width at the base about 35 ns. The input impedance of the amplifier should be about 300Ω , and cross-talk between neighboring channels less than 0.5%.

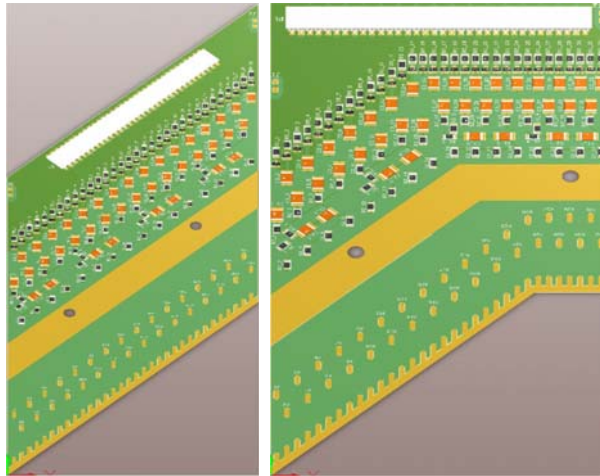


Fig. 9. General view of two MBs: one for the left inclined side and the other for the left corner zone of the module prototype

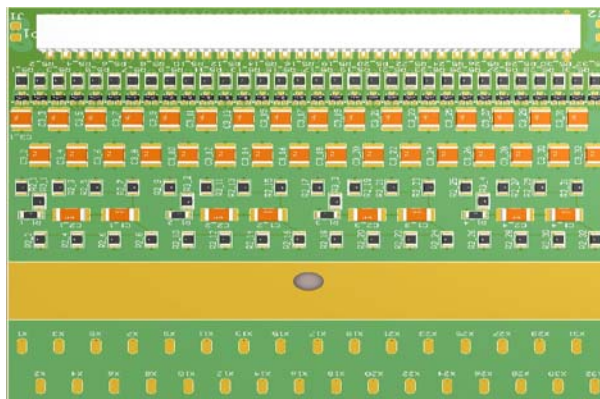


Fig. 10. General view of the MB for the central zone of the prototype

1.4. Intrinsic Straw Detector Parameters. The straw diameter was chosen as a reasonable compromise between the speed of response, number of detecting elements and value of the occupancy.

The current MUCH straw subsystem design is based on straw tubes with a diameter of 6 mm. The tube parameters (60 ns maximum drift time and 35 ns pulse duration), as well as maximum value of the occupancy ($< 7\%$) in central Au–Au collisions (as found from Monte Carlo simulations), are in good match with the maximum 10 MHz rate of Au–Au collisions at 25A GeV in the CBM setup [1]. However, even though these parameters seem to be adequate for the expected running conditions, a possibility to adapt the straw detector concept to the cases where a higher granularity is required was studied and confirmed [7–10]. The beam test of the prototype with a granularity of 4 cm^2 had shown that its time and spatial parameters do not differ from those of conventional tracking detectors based on drift

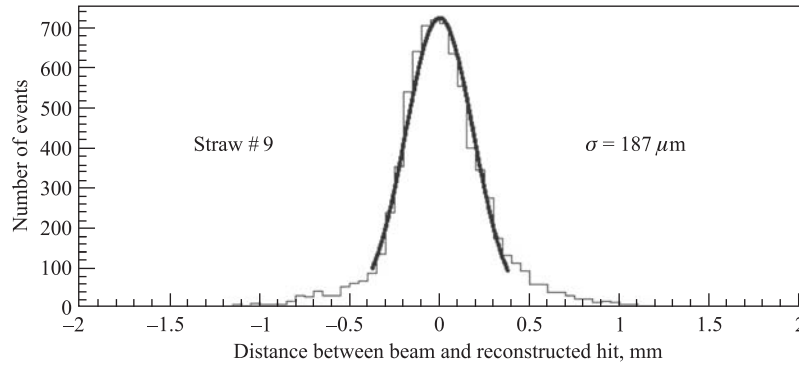


Fig. 11. Difference of coordinates measured in the 4 mm straw tube and predicted at the tube position using the track reconstructed in silicon detectors

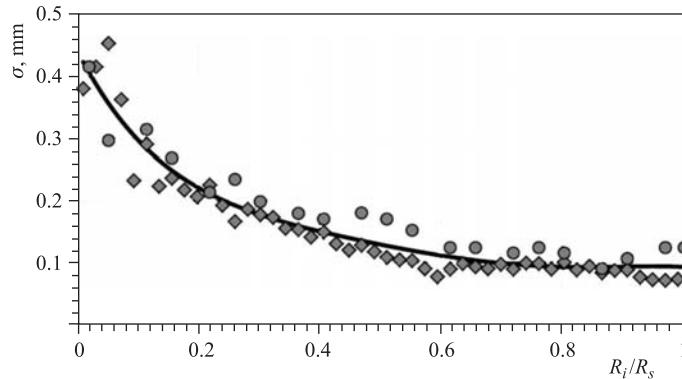


Fig. 12. Spatial resolution as a function of the scaled distance to the anode for the straws with 4 mm (circles) and 9.53 mm (diamonds) inner diameter. The straws were blown with the gas mixture Ar/CO₂ (80/20), and the gas gain was about $7 \cdot 10^4$ in both cases

tubes [11–13]. The developed method for manufacturing straw coordinate detectors makes it possible to achieve a granularity as fine as 1 cm² with the straw full length up to 4 m.

The straws with inner diameters of 4 and 9.53 mm have been tested in the SPS test beam at CERN, with the same gas mixture (Ar/CO₂ (80/20)) and the gas gain $\sim 7 \cdot 10^4$ in both cases. The efficiency was about ~ 98 and 99% for the 4 and 9.53 mm straws, respectively. Figure 11 shows the typical distribution of the deviations of the measured particle coordinates from those corresponding to the tracks reconstructed using the data from pad silicon detectors.

The spatial resolution for the 9.53 and 4 mm straws as a function of the scaled distance to the anode (normalized to the tube inner radius) is shown in Fig. 12 [14]. In both cases these dependences can be well described by a single curve ($\chi^2/\text{ndf} = 0.94$). The observed universality of the dependence makes it possible to predict the coordinate resolution for the straws with different diameters given the operation parameters are similar (gas composition and gas gain). It also simplifies the task of track fitting by providing the error parametrization curve. The spatial resolution changes from ~ 450 to $\sim 80 \mu\text{m}$ near the anode and cathode,

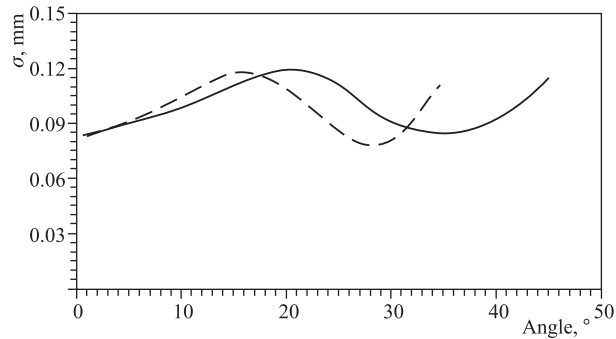


Fig. 13. The effective average value of the spatial resolution of a double layer chamber as a function of the particle incident angle. The dashed and solid lines are for the distances between the anode planes of the chamber 10.7 and 13.7 mm, respectively. Tube diameter is 9.53 mm

respectively. Each chamber of MUCH has two straw layers, and one layer is shifted by half a diameter with respect to the other in order to resolve left-right ambiguities and to obtain single track efficiency for a double layer above 99%. The double layer arrangement also helps to efficiently combine the radial resolution dependences of two layers. A simple estimate shows that in this case the effective averaged spatial resolution of a two layer chamber will be from 90 to 120 μm in a wide range of the particle incident angles (Fig. 13).

2. DETECTOR PERFORMANCE SIMULATION

2.1. Geometry. Currently there exist two alternative MUCH configurations for SIS-300, described in Monte Carlo: the homogeneous one based on GEM detectors with pad readout in all tracking stations [15] and GEM + straw one presented above. At present, the heterogeneous muon system setup description (Fig. 1) does not include some details, e.g., the realistic modular station structure is not fully implemented and only the «square-tube» approximation is used. However, these (intentional) omissions do not introduce any significant bias into the simulation results, making at the same time easier the comparison of these two configurations.

2.2. Detector Occupancy. The detector occupancy (average number of hits per event per tube) was estimated from the Monte Carlo event sample of UrQMD central Au + Au collisions at 25A GeV. The obtained results are shown in Fig. 14 for straw tubes with a diameter of 6 mm. One can see that the maximum occupancy does not exceed 7% and should not present any problems for pattern recognition.

2.3. Detector Response Simulation. The choice of the detector configuration should be based on realistic simulation of the detector response. For straw tubes the most important features relevant for the physics performance are the hit merging and left-right ambiguity. The first one describes the fact that the straw tube does not have a multi-hit capability; i.e., in case when more than one particle pass through the tube, only one of them (closest to the anode wire) is detected. The second feature takes into account the straw tube inability to distinguish drift direction, i.e., to determine whether particle passes to the left or right from the anode wire. Both features can easily be implemented during the simulation at the hit production level and were included in the studies below.

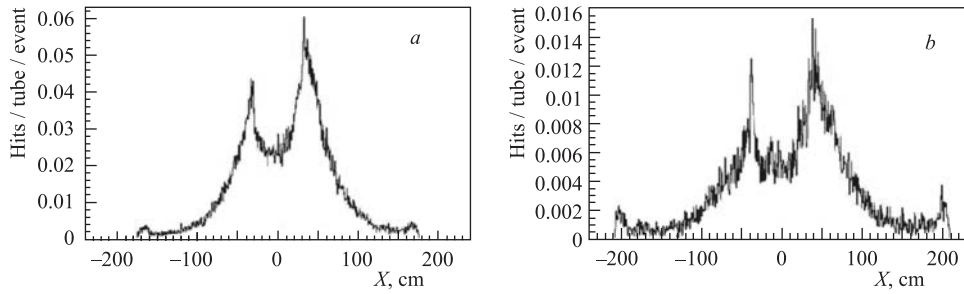


Fig. 14. Transverse occupancy profiles of straw tube stations for Au + Au central collisions at 25A GeV. a) Station 4; b) station 5

2.4. Tracking Performance. The tracking performance studies were based on a comparison of the tracking results for two alternative MUCH configurations: all-GEM and GEM+straw one. The homogeneous detector presumably should provide better conditions for track reconstruction algorithms, therefore giving a good reference point for comparative studies.

The studies were performed for muons with a momentum of 2.5–25 GeV/c and a polar angle of 2.5–25° embedded into UrQMD central Au + Au collisions at 25A GeV. The track reconstruction algorithm was based on STS track propagation through the muon system [16]. The obtained results are presented in Table 2. As can be seen, both MUCH configurations demonstrate similar performance when the tracking algorithm properly takes into account the detector features (note efficiency restoration for GEM + straw when the track branching is used). The higher ghost activity in this case can also be explained by some deficiencies (lack of proper tuning) in the algorithm as can be seen in the next Section.

Table 2. Track reconstruction efficiency and ghost activity obtained with two tracking algorithm modifications: nearest neighbour (NN) and branching

Geometry	Efficiency, %		Ghosts (tracks/event)	
	NN	Branch	NN	Branch
GEM	95.2	95.6	3.7	3.6
GEM+straw	89.8	95.0	3.9	9.3

2.5. Trigger Performance. The emission of lepton pairs out of the hot and dense collision zone of heavy-ion reactions is a promising probe to study the electromagnetic structure of hadrons under extreme conditions. The reconstruction of vector mesons ($\rho, \omega, \phi, J/\psi, \psi'$) is one of the prime tasks of the CBM experiment. The proposed muon system is intended to do this study using a dimuon decay mode.

Since the dimuon yield from vector meson decays is expected to be very low, it is essential to develop a fast and efficient trigger for such events.

The muons from decays of low-mass vector mesons (LMVM), e.g., ω , will be rather soft, making it undesirable to use the total absorber thickness. Therefore, the detector stations surrounding the last but one absorber should be used in the trigger in a manner described in [17]. Here somewhat different aspects of this problem are addressed.

As in the case of the tracking performance analysis, for the LMVM trigger study both the alternative MUCH configurations were considered in order to compare their ability to do the

job. It was also useful to obtain a tool independent of the general tracking to compare two detector configurations (keeping in mind that the general tracking might not be fully tuned to properly handle the heterogeneous detector environment).

The following event selection strategy was used:

- find track segments in stations 4 and 5;
- merge track segments from different stations taking into account the multiple scattering in the absorber;
- propagate track to the target position using linear extrapolation;
- apply a cut on radial position of the extrapolated points;
- accept event if two or more tracks pass the cuts.

In order to ensure a fair comparison of the two detector configurations, the following implementation details were considered:

- simplified (planar) GEM geometry: automatic segmentation and simple digitization and hit finding;
- 6 mm straw tubes: hit producer with hit merging (i.e., only one hit per tube is kept) and left-right ambiguity (i.e., for each «true» hit a mirror one (symmetric relative to anode wire position) is added (no local left/right ambiguity resolution);
- track segments should include the maximum number of hits (i.e., 3 for GEMs and 6 for straws);
- segment merging: introduced multiple scattering parameters $\sigma_{\alpha\beta}$ and σ_{xy} (thick scatterer approximation) which were obtained from simulation.

The trigger efficiency and background rejection factor were estimated on Monte Carlo event samples of UrQMD central Au+Au events at 25A GeV mixed with $\omega \rightarrow \mu\mu$ decays and minimum bias events, respectively. The obtained results are presented in Table 3. One can see that both detector configurations demonstrate the similar performance.

Table 3. Trigger efficiency for the dimuon signal and background rejection factor

Geometry	Efficiency, %	Background rejection
GEM	6.7 ± 0.4	19.8
Straws	6.7 ± 0.4	19.7

2.6. Future Developments. The concept of the straw tube system utilization in CBM MUCH still needs some additional work on its improvement and refinement. The following issues require further attention:

- Pattern recognition with free-streaming data. Since the maximum drift time in straw tubes will be ~ 60 ns, the time acceptance window for pattern recognition with time stamped data should be of a similar value. For high intensity running, the ability to successfully match the data should be checked.
- Necessity (and possibility) of drift time measurements. Preliminary studies show that during the offline reconstruction the hit localization in the tube center is satisfactory. On the other hand, the LMVM trigger would benefit from the drift time measurement, making it necessary to develop an approach to extract the start time t_0 from the straw tube information itself.

- Geometry optimization. The current station configuration (3 doublets at 0 and $\pm 10^\circ$) seems to work fine. However, adding one more double layer would provide some reasonable redundancy (especially important for t_0 determination). The stereo angles in station 5, where the occupancy is low, could be increased in order to improve resolution in vertical direction.

- Track reconstruction. While the present approach to track reconstruction seems to give sufficiently good results, there is an indication that the heterogeneous tracking environment imposes some limitations on the flexibility, making the detector optimization task rather difficult. That is why it looks reasonable to try to factorize the problem, i.e., to develop some «pre-tracking» procedure in the straw tube subsystem, which will create track segments (tracklets) and perform some candidate preselection before including them into the general tracking.

Acknowledgements. The authors would like to thank Drs. P. Senger, W. Müller, A. Kiseleva and A. Lebedev (GSI, Darmstadt, Germany) for many useful discussions.

REFERENCES

1. Compressed Baryonic Matter Experiment Technical Status Report. 2005.
2. *Bychkov V. et al.* JINR Commun. P13-98-269. Dubna, 1998.
3. *Bychkov V. et al.* // Part. Nucl., Lett. 2002. No. 2 [111]. P. 64–73.
4. *Bychkov V. et al.* // Nucl. Instr. Meth. A. 2006. V. 556. P. 66–79.
5. *Abbon P. et al.* // Nucl. Instr. Meth. A. 2007. V. 577. P. 455–518.
6. *Bevensee B. et al.* // IEEE Trans. Nucl. Sci. 1996. V. 43, No. 3. P. 1725.
7. *Peshekhonov V. et al.* CBM Progress Report 2008. GSI Report 2009-03. Darmstadt, 2009. P. 35.
8. *Boguslavskiy I. et al.* CBM Progress Report 2009. GSI Report 2010-03. Darmstadt, 2010. P. 29.
9. *Davkov K. et al.* // Nucl. Instr. Meth. A. 2008. V. 584. P. 285.
10. *Davkov V. et al.* // Part. Nucl., Lett. 2007. No. 4 (140). P. 545.
11. *Gusakov Yu. V. et al.* // Part. Nucl., Lett. 2010. V. 7, No. 12. P. 132.
12. *Bazylev S.N. et al.* // Nucl. Instr. Meth. A. 2011. V. 632. P. 75.
13. *Davkov V.I. et al.* // Ibid. V. 634, No. 1. P. 5.
14. *Dikusar N.L. et al.* The Spatial Resolution of Two-Layer Coordinate Detectors Based on Thin-Walled Drift Tubes // Part. Nucl., Lett. (submitted).
15. *Bhaduri P.P. et al.* MUCH Layout Optimization for SIS-100. CBM Progress Report 2010. Darmstadt, 2011. P. 34.
16. *Lebedev A. et al.* Status of Tracking in the TRD and MUCH Detectors of the CBM Experiment. CBM Progress Report 2010. Darmstadt, 2011. P. 72.
17. *Kiseleva A. et al.* A Di-muon Trigger for CBM. CBM Progress Report 2009. Darmstadt, 2010. P. 67.

Received on July 7, 2011.